Differential Effects of General Anesthetics on the Quaternary Structure of the Ca-ATPases of Cardiac and Skeletal Sarcoplasmic Reticulum†

Howard Kutchai,*,‡ Lisa M. Geddis,‡ Larry R. Jones,§ and David D. Thomas*,||

Department of Molecular Physiology and Biological Physics, University of Virginia, Charlottesville, Virginia 22908, Krannert Institute of Cardiology, Department of Medicine, Indiana University School of Medicine, Indianapolis, Indiana 46202, and Department of Biochemistry, University of Minnesota Medical School, Minneapolis, Minnesota 55455

Received September 5, 1997; Revised Manuscript Received December 22, 1997

ABSTRACT: The effects of the general anesthetics hexanol, halothane, and diethyl ether on Ca-ATPase activity and on the oligomeric state of the Ca-ATPase of sarcoplasmic reticulum (SR) from cardiac and skeletal muscle were investigated. The effects of these general anesthetics on Ca-ATPase activity were similar in cardiac and skeletal SR and were characterized by stimulation of Ca-ATPase activity at lower concentrations of anesthetics and inhibition at higher concentrations. The distribution of the Ca-ATPase among its oligomeric states was estimated from the time-resolved phosphorescence anisotropy (TPA) decay of SR in which Ca-ATPase was covalently labeled with erythrosin isothiocyanate (ERITC) or with erythrosin iodoacetamide (ERIA). In contrast to the similar responses of Ca-ATPase activity, there were marked differences in the responses to general anesthetics of the TPA decay between cardiac and skeletal SR. In *cardiac* SR hexanol, halothane, and diethyl ether caused pronounced increases in the limiting anisotropy at very long times (r_∞), which indicate increases in the fraction of oligomers too large to rotate on the millisecond time scale of the experiments. In *skeletal* SR, by contrast, there were no significant changes in r_∞ in response to the three general anesthetics. This difference between cardiac and skeletal SR in response to general anesthetics is not due to the presence of phospholamban in cardiac SR, since SR from AT-1 cells, which have the SERCA2a isoform of Ca-ATPase, but only trace levels of phospholamban, have increases in r_∞ in response to the general anesthetics that resemble those in cardiac SR. Experiments with cardiac SR labeled with ERIA give similar results, showing that the results with ERITC are not an artifact of the labeling procedure. Increasing the ionic strength with LiCl diminished the proportion of large immobile oligomers of cardiac Ca-ATPase under control conditions but enhanced the formation of large oligomers in response to hexanol.

Several previous studies from this laboratory have dealt with the relationship between the oligomeric state of the Ca-ATPase of sarcoplasmic reticulum and its ATPase activity (reviewed in ref *1*). We have studied the effects of membrane thickness (*2*), the influence of general and local anesthetics on SR[1] from skeletal muscle (*3*−*6*) and SR from cardiac muscle (*7*), the effects of melittin (*8*−*11*), the influence of inhibitors of Ca-ATPase (5, *12*), and the effects of phospholamban in cardiac SR (*13*, *14*) on the quaternary structure and enzymatic activity of the Ca-ATPase.

In these previous studies, the major means of assessing the distribution of the Ca-ATPase among its oligomeric states has been measurements of the time-resolved phosphorescence anisotropy (TPA) decay of erythrosin isothiocyanate (ERITC) covalently bound to Ca-ATPase (*3*). Previous studies from this laboratory found that conditions that promote the formation of larger oligomers of the Ca-ATPase are associated with decreased ATPase activity of both skeletal and cardiac SR. Several studies have described significant differences between skeletal and cardiac SR (*5*, *13*, *14*), but in both preparations, we have found that conditions that lead to an increase in the limiting phosphorescence anisotropy at very long times (r_∞) of ERITC-labeled SR, which indicates an increase in the fraction of oligomers too large to rotate on the millisecond time scale, have correlated with conditions that lead to greatly diminished ATPase activity.

We have previously noted qualitative differences in the responses of the Ca-ATPases of skeletal and cardiac SR to halothane (*5*, *7*, *15*). The aim of the present study is to directly compare SR from cardiac and skeletal muscle in the responses of oligomeric state and ATPase activity to general anesthetics. We have found that cardiac and skeletal SR are rather similar in the responses of Ca-ATPase activity to the general anesthetics hexanol, halothane, and diethyl ether. By contrast, the TPA decays of ERITC- and ERIA-labeled cardiac SR Ca-ATPase are affected quite differently from those of ERITC-labeled skeletal SR by general anesthetics.

† This work was supported by grants from the National Institutes of Health: GM27906 (D.D.T.); HL49428 and HL06308 (L.R.J.); GM50764 (H.K.).

* To whom correspondence should be addressed.
‡ University of Virginia.
§ Indiana University.
|| University of Minnesota Medical School.

[1] Abbreviations: SR, sarcoplasmic reticulum; MOPS, 3-(*N*-morpholino)propanesulfonic acid; ATP, adenosine triphosphate; EGTA, ethylene glycol bis(β-aminoethyl ether)-*N*,*N*,*N*′,*N*′-tetraacetic acid; TPA, time-resolved phosphorescence anisotropy; DMF, *N*,*N*-dimethylformamide; NADH, β-nicotinamide adenine dinucleotide, reduced form; ERITC, erythrosin 5-isothiocyanate; ERIA, erythrosin 5-iodoacetamide.

S0006-2960(97)02200-9 CCC: $15.00
Published on Web 02/04/1998

The most striking difference is that r_∞ increases markedly in response to general anesthetics in ERITC-labeled cardiac SR but not in ERITC-labeled skeletal SR. This suggests that these general anesthetics induce the formation of large Ca-ATPase oligomers in cardiac SR but not in skeletal SR. The major purposes of this study are to more completely characterize the different responses of cardiac and skeletal SR to general anesthetics and to investigate possible explanations for the differences.

MATERIALS AND METHODS

Reagents and Solutions. ERITC and ERIA were obtained from Molecular Probes (Eugene, OR) and stored in DMF under liquid nitrogen. The calcium ionophore A23187 was obtained from Calbiochem (San Diego, CA). Unless stated otherwise, ATPase assays and spectroscopic measurements were carried out at 25 °C in a standard buffer containing 50 mM imidazole (pH 7.0), 100 mM KCl, 5 mM $MgCl_2$, and 0.2 mM EGTA, with or without added $CaCl_2$ required to reach the desired concentration of free Ca^{2+}. The concentration of free Ca^{2+} was calculated as described previously (*13*, *16*).

Preparations. Skeletal sarcoplasmic reticulum was prepared (*17*) from fast twitch muscle of New Zealand White rabbits. Cardiac sarcoplasmic reticulum prepared from canine ventricular tissue (*18*) was kindly provided by Dr. Joseph J. Feher. Atrial tumor cell SR was prepared (*19*) from AT-1 atrial myocytes (*20*). SR from AT-1 myocytes has levels of SERCA2a Ca-ATPase similar to those in SR from ventricular cells but contains only traces of phospholamban (*21*). Protein concentrations were determined by the biuret method (*22*) using bovine serum albumin as standard.

ATPase Assays. Ca-ATPase activity was assayed by an enzyme-linked, continuous ATPase assay (*23*) at 25 °C. The assay volume was 0.94 mL, and we used 3.75 μg of skeletal SR or 15 μg of cardiac SR in an assay mixture containing 2.5 mM $(Na)_2$ATP, 0.5 mM phosphoenolpyruvate, 0.25 mM NADH, 10 IU of pyruvate kinase, and 10 IU of lactate dehydrogenase. The assay mixture also contained 1 μg/mL of the ionophore A23187 to prevent a buildup of Ca^{2+} inside the vesicles that might inhibit the Ca-ATPase activity. When an anesthetic was used, it was added to the assay mixture before the SR and the SR was allowed to preincubate with anesthetic in assay mixture for 20 min at room temperature before the reaction was started. The absorbance of NADH was recorded at 340 nm to determine the rate of ATP hydrolysis in the absence of Ca^{2+}. Then the assay was started by adding the amount of $CaCl_2$ required to give the desired free [Ca^{2+}] and the rate of ATP hydrolysis determined from the rate of change of the absorbance at 340 nm.

Labeling of Ca-ATPase with ERITC or ERIA. For time-resolved phosphorescence experiments, Ca-ATPase-containing SR from skeletal SR, cardiac SR, or AT-1 cardiomyocyte SR was labeled with ERITC (*3*) or with ERIA (*24*). In all cases, the number of moles of ERITC or ERIA added was 0.9 times the estimated number of moles of Ca-ATPase present, computed by assuming that Ca-ATPase accounts for 75% of the protein in skeletal SR and for 25% of the protein in cardiac SR and in AT-1 cardiomyocyte SR. The buffer for ERITC labeling was 100 mM KCl, 5 mM $MgCl_2$, and 30 mM Tris, pH 8.7, and that for labeling with ERIA was 100 mM KCl, 5 mM $MgCl_2$, and 30 mM MOPS, pH 7.0. The SR protein concentration was 5 mg/mL, and the labeling reaction was allowed to proceed at room temperature for 20 min in the dark. Then the samples were diluted 10-fold with ice-cold pH 7.0 buffer and centrifuged at 66000*g* for 10 min to pellet the SR. SR samples were resuspended in at 10 mg/mL in 50 mM imidazole (pH 7.0) and 0.3 M sucrose and kept on ice in the dark. To determine which proteins in SR are labeled with ERITC or ERIA, labeled preparations were subjected to SDS−polyacrylamide gel electrophoresis, the gels were scanned with a Fluorimager (Model 595, Molecular Dynamics, Sunnyvale, CA), and the data obtained were analyzed with Image-Quant software (Molecular Dynamics).

Time-Resolved Phosphorescence Anisotropy (TPA) Data Collection. Prior to the acquisition of phosphorescence data, an aliquot of labeled SR was diluted to a concentration of 0.25−0.50 mg of protein/mL in the standard buffer with the appropriate amount of $CaCl_2$ in a stoppered fluorescence cuvette. Oxygen was removed from the sample by the addition to the cuvette of 200 μg/mL glucose oxidase, 30 μg/mL catalase, and 5 mg/mL β-D-glucose (*25*); then the cuvette was flushed with N_2 and tightly stoppered. Deoxygenation was allowed to proceed for at least 20 minutes prior to data collection. Anesthetic, when used, was present in the buffer, and there was a preincubation period of 20−30 min with anesthetic before data collection was begun. After about 20 min, the data obtained did not depend significantly on the preincubation time.

When halothane was used, in either Ca-ATPase assays or TPA determinations, the cuvette was completely filled with the assay solution, including SR. Then halothane, diluted 1:10 (v/v) in DMF, was added, the cuvette was sealed with its Teflon stopper, and the contents were mixed by repeated inversion.

The anisotropy is defined as

$$r(t) = \frac{I_{vv} - GI_{vh}}{I_{vv} + 2GI_{vh}} \quad (1)$$

where I_{vv} and I_{vh} are the vertical and horizontal components, respectively, of the emission after excitation with a vertically polarized pulse. TPA decays were recorded using an instrument described previously (*26*), by signal averaging the time-dependent phosphorescence decays with a single detector and a polarizer that alternates between vertical ($I_{vv}(t)$) and horizontal ($I_{vh}(t)$) orientation every 2000 laser flashes. The laser firing rate was 200 Hz; a typical $r(t)$ acquisition run required about 4.5 min to complete the 10 loops or cycles of 4000 laser pulses per loop (2000 in each orientation of the polarizer). G is an instrumental correction factor, determined by measuring the anisotropy of a solution of eosin-labeled bovine serum albumin in 90% glycerol at 25 °C and calculating the value of G in eq 1 required to give an anisotropy value of zero, the theoretical value for a isotropically tumbling chromophore.

Data Analysis. TPA decays were analyzed (*3*) by fitting them according to a multiple-exponential-decay equation.

$$\frac{r(t)}{r(0)} = \sum_{i=1}^{3} A_i e^{-t/\phi_i} + A_\infty \quad (2)$$

where ϕ_i, the rotational correlation time of the ith rotating component, is inversely proportional to the rotational diffusion coefficient D_i, A_i is proportional to the mole fraction of Ca-ATPase with a correlation time ϕ_i, and A_∞ is the normalized final anisotropy (r_∞/r_0).

Equation 2 was fit to experimental TPA decay data using the nonlinear least-squares algorithm of Marquardt (*27*). The quality of the fit was gauged by comparing χ^2 values and by evaluating the residuals. Previous reports from this laboratory (*3*, *7*, *12*) have shown that the TPA of ERITC-SR is dominated by the uniaxial rotational diffusion of the labeled Ca-ATPase about an axis normal to the bilayer and that the TPA decays are fit well by a sum of three exponentially decaying terms plus a constant term.

In the present study, we have also fit TPA data to an analytical uniaxial rotation model (*28*) that explicitly incorporates all of the factors that determine the anisotropy decay kinetics of uniaxially rotating chromophores:

$$r(t) = \sum_{i=1}^{n} f_i r_i(t) + f_l r(0) \tag{3}$$

where f_i is the mole fraction associated with the ith rotating species and f_l is the mole fraction of Ca-ATPase that does not rotate on the time scale of the experiment (immobile Ca-ATPase). Using this expression, changes in the mole fraction of immobile Ca-ATPase induced by SR perturbants can be directly determined, independent of the orientation of the probe (*12*).

The expression for the individual anisotropy of the ith uniaxially rotating species (*29*) is

$$r_i(t) = \kappa(a_1 e^{-D_i t} + a_2 e^{-4D_i t} + a_3) \tag{4}$$

where

$$a_1 = 1.2(\sin\theta_a \cos\theta_a \sin\theta_e \cos\theta_e \cos\phi_{ae}) \tag{5a}$$

$$a_2 = 0.3(\sin^2\theta_a \sin^2\theta_e \cos 2\phi_{ae}) \tag{5b}$$

$$a_3 = 0.2(3\cos^2\theta_a - 1)(3\cos^2\theta_e - 1) \tag{5c}$$

Here D_i is the rotational diffusion coefficient about an axis normal to the plane of the membrane, θ_a and θ_e are respectively the angles between the probe's absorption and emission dipoles and the membrane normal, ϕ_{ae} is the azimuthal angle between the absorption and emission transition dipoles of the probe, and κ is the order parameter for fast (submicrosecond) motion of the probe with respect to the protein. The submicrosecond motion may result from the site of probe attachment undergoing segmental motion or from partial freedom of motion of the probe itself around its site of attachment.

The uniaxial rotation model (eqs 3−5) accounts for (a) the biexponential decay of each species (eq 4), (b) the order parameter for submicrosecond motion, κ, and (c) the angular dependence of the amplitudes of the exponentially decaying terms (eqs 5a−c). We have observed previously that TPA decays of ERITC-labeled skeletal and cardiac SR are best fit by including three uniaxially rotating species (*7*, *12*). Each species is assumed to have the same values of θ_a, θ_e, and ϕ_{ea} and to differ from the other species only in its diffusion coefficient, presumably due to differences in aggregation state. Fitting the uniaxial rotation model to our data was done using a nonlinear least-squares fitting routine employing the Marquardt−Levenberg algorithm in a computer program developed by Roberta Bennett and Joseph Mersol of this laboratory.

RESULTS

Specificity of Labeling Skeletal and Cardiac Ca-ATPases with ERITC and ERIA. Scans of the fluorescence intensity of gels of skeletal and cardiac SR labeled with ERITC and ERIA are shown in Figure 1. In both cardiac and skeletal SR, the principal protein labeled with ERITC comigrated with the band identified as Ca-ATPase (Figure 1A,B). In cardiac SR, there was only slightly more ERITC fluorescence that is not associated with the Ca-ATPase than was the case in skeletal SR.

ERIA (Figure 1C,D) labeled Ca-ATPase with somewhat less specificity than did ERITC, especially in cardiac SR (Figure 1D). Although the Ca-ATPase is the most heavily labeled protein in cardiac SR, a number of other protein bands are significantly labeled in this preparation.

Influence of Hexanol on Decay of Phosphorescence Anisotropy of ERITC-labeled Cardiac and Skeletal SR. ERITC-labeled cardiac SR was preincubated at pCa 5.5 in the standard buffer alone or in standard buffer with 10, 20, 25, or 30 mM hexanol for 20−30 min before the phosphorescence anisotropy measurements were begun. Hexanol, at concentrations above 10 mM, caused significant slowing of the decay of phosphorescence anisotropy and resulted in an increase in r_∞, the final anisotropy (Figure 2A**)**.

These results were in marked contrast to our previous experiments on the effects of hexanol on ERITC-labeled skeletal SR (*6*). Since the experimental conditions, including the free [Ca^{2+}], in the earlier study were somewhat different from those employed here, additional experiments were performed with ERITC-labeled skeletal SR under the same conditions as those employed in the experiments of Figure 2A. The results of these experiments with ERITC-labeled skeletal SR (Figure 2B) are consistent with our earlier studies. Preincubation with 10 or 20 mM hexanol resulted in faster decay of the phosphorescence anisotropy, while preincubation with 30 or 40 mM hexanol slowed the decay. At all concentrations of hexanol employed, there were no significant changes in r_∞, in marked contrast to our results with cardiac SR (Figure 2A). The major purpose of this study is to investigate this difference in TPA response between cardiac and skeletal SR.

Description of the Effects of Hexanol on TPA of ERITC-labeled Cardiac SR by the Uniaxial Rotation Model. To obtain a more quantitative description of the TPA response of ERITC-labeled cardiac SR to hexanol, the uniaxial rotation model (eqs 3−5) was fit to the data of Figure 2A. Results of the fitting are shown in Figure 3. With increasing [hexanol], there were progressive decreases in the computed values of f_1 and f_2, the mole fractions of the fastest-rotating (smallest) and intermediate-sized rotating species, respectively, and a progressive increase in f_l, the mole fraction of very large, immobile oligomers (Figure 3A). The mole fraction of the slowest (largest) rotating species, f_3, changed only slightly with increasing [hexanol]. The computed

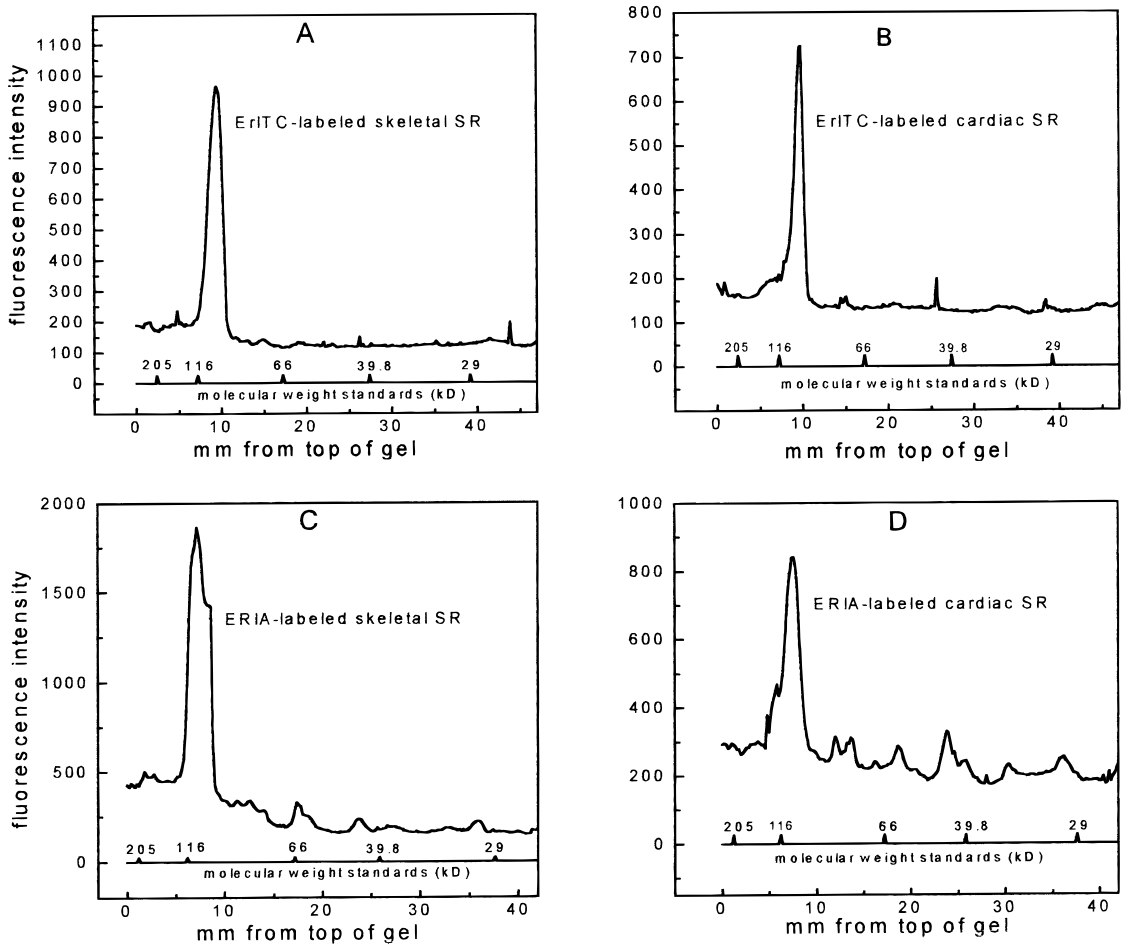

FIGURE 1: Scans of SDS−PAGE gels of (A) ERITC-labeled skeletal SR and (B) ERITC-labeled cardiac SR and of (C) ERIA-labeled skeletal SR and (D) ERIA-labeled cardiac SR. Skeletal and cardiac SR's were labeled with ERITC or ERIA as described under Materials and Methods. The labeled SR preparations were subjected to SDS polyacrylamide gel electrophoresis (*61*) on 10% acrylamide gels. The fluorescence of the gels was quantified using a Fluorimager (Molecular Devices), and the figure shows line scans of the fluorescence data produced with Image-Quant software (Molecular Devices).

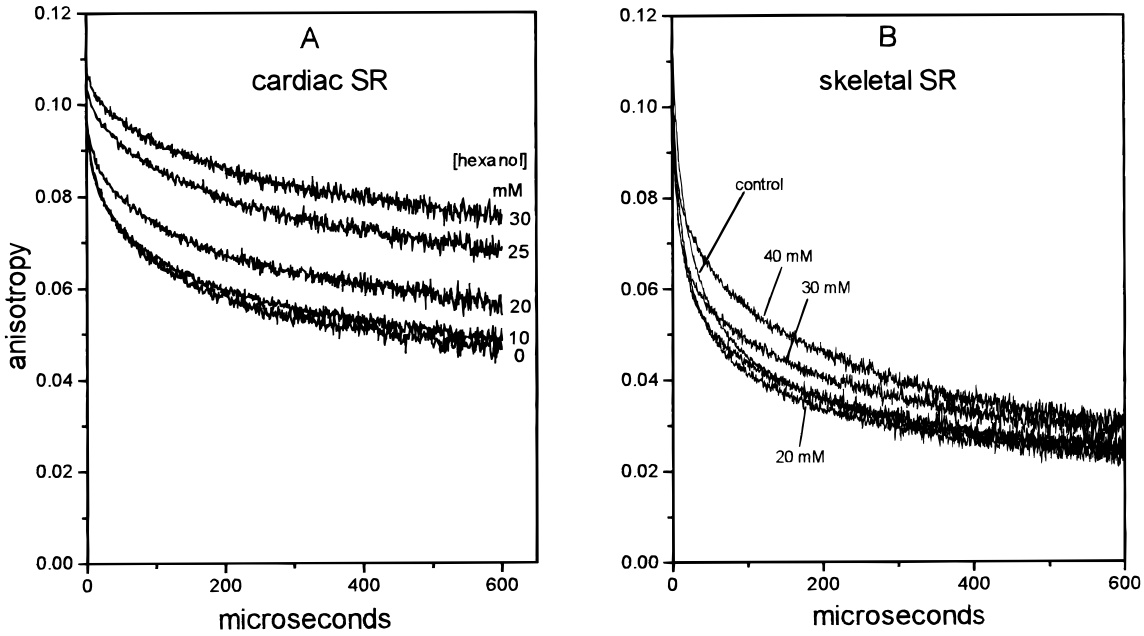

FIGURE 2: Influence of hexanol on phosphorescence anisotropy decay of ERITC-labeled cardiac SR (A) and ERITC-labeled skeletal SR (B). In panel B, the one curve that does not have a pointer is for 10 mM hexanol (this curve is close to the 20 mM curve at early times and close to the control curve at later times).

values of D_1, the rotational diffusion coefficient of the fastest-rotating species, decreased slightly with increasing hexanol concentration (Figure 3B). The computed values of D_2 and D_3, the rotational diffusion coefficient of the intermediate

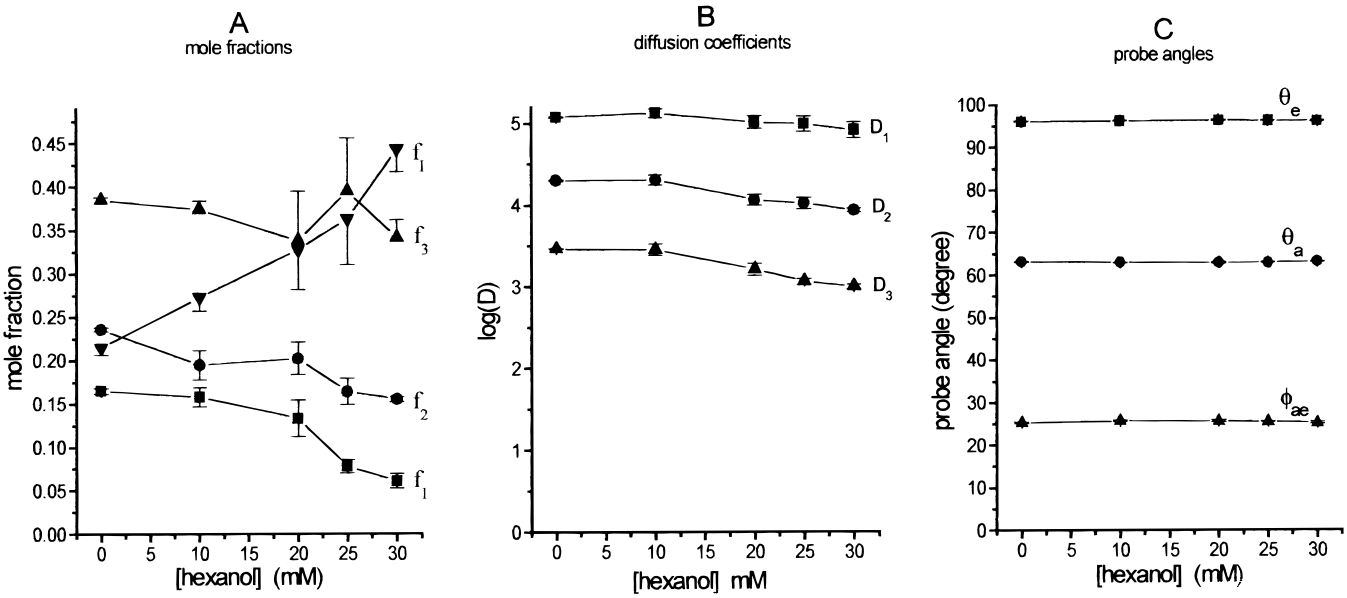

FIGURE 3: Values of parameters computed using the unconstrained uniaxial model. The uniaxial rotation model (eqs 3−5) was fit to the data of Figure 2A. Shown are (A) computed values of the mole fractions (*f*) of the different species, (B) computed values of the rotational diffusion coefficients (*D*) of the three rotating components, and (C) computed values of the three probe angles. The error bars indicate the standard deviations obtained from fitting the average of four to six separate phosphorescence anisotropy decay curves for each concentration of hexanol.

and slowest-rotating components, decreased more substantially with increasing [hexanol]. The fits yielded probe angles, θ_a, θ_e, and ϕ_{ae} (Figure 3C), that did not change significantly with increasing [hexanol]. The errors in the computed angles were much less than errors in the values of the *f* 's and the *D*'s: the average standard deviation of the computed angles over all the hexanol concentrations was 0.1°. The decreases in the values of D_2 and D_3 suggest that the average sizes of the oligomers in these classes may be increasing with increasing [hexanol]. The initial guesses for the values of the *f* 's, *D*'s, and the three probe angles could be varied substantially with little effect on the parameter values to which the fitting routine converged.

These results are consistent with the interpretation that that the large increase in r_∞ that occurs in cardiac SR in response to hexanol is due to an increase in the fraction of oligomers that are too large to rotate on the time scale of the experiment, rather than to changes in the probe angles. However, the values of the parameters computed with the uniaxial model (Figure 3) may not be unique fits to the experimental data. We asked whether the large changes in the anisotropies at long times with increasing [hexanol] might be fit just as well by changes in the probe angles. We fit the uniaxial model to the data of Figure 2A while keeping f_l constant at the value computed for zero hexanol. In this case, the model fit the data by adjusting the values of f_1, f_2, f_3, and the three diffusion coefficients but yielded values of the three probe angles that were not significantly different from the values computed with unconstrained values of f_l. The values of χ^2 for the fits with f_l held constant averaged 6.5% greater than those for fits where f_l was allowed to vary. Then we fit the data with the uniaxial model with all the amplitudes (f_1, f_2, f_3, and f_l) fixed at the values computed for zero hexanol. With these constraints, the model was still able to fit the experimental data quite well, albeit with still higher χ^2 values, by adjusting the computed values of the probe angles.

The fact that the unconstrained model fits the data by increasing f_l, while keeping the probe angles constant, is consistent with the interpretation that the large increases in r_∞ that occur in cardiac SR in response to hexanol are due to increases in the mole fraction of very large oligomers, rather than to changes in the probe angles. However, since the experimental data can be fit quite well by the uniaxial model with the mole fractions held constant, resulting in changes in the computed probe angles, our results cannot be regarded as unequivocal support for the interpretation that the probe angles do not change. On the other hand, if there are multiple oligomeric species of Ca-ATPase in the SR membrane, to require that the mole fractions of all these species remain invariant seems to us an unrealistically stringent constraint.

Influence of Phospholamban on the Response of ERITC-labeled Cardiac SR to Hexanol. The regulatory protein phospholamban (*30*−*33*) is present in cardiac SR, but absent from the SR, of fast skeletal muscle. To inquire whether phospholamban is responsible for the different responses to hexanol of ERITC-labeled cardiac SR, we determined the effects of hexanol on ERITC-labeled SR from AT-1 atrial myocytes (*20*) that express the SERCA2a (cardiac) isoform of Ca-ATPase in their SR but express phospholamban only at trace levels (*21*). SR prepared from AT-1 atrial myocytes was labeled with ERITC, and phosphorescence experiments were done under the same conditions as those employed in the experiments of Figure 2A,B. Preincubation with hexanol at 10 mM had no significant effect on the anisotropy decay, but 20 and 30 mM hexanol caused a slowing of the decay of phosphorescence anisotropy and a significant increase in the final anisotropy (Figure 4). The behavior of the atrial tumor cell SR in response to hexanol resembles that of cardiac SR (Figure 2A).

These data support for the conclusion that the presence of phospholamban in cardiac SR is not responsible for the

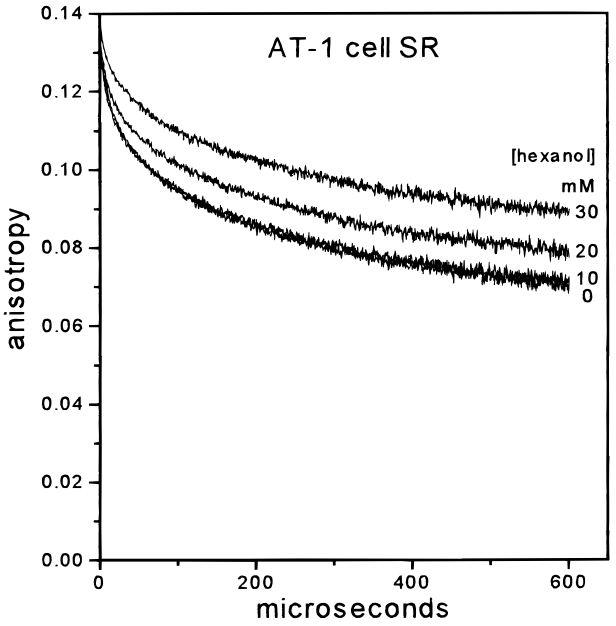

FIGURE 4: Influence of hexanol on phosphorescence anisotropy decay of ERITC-labeled SR from AT-1 cardiomyocytes.

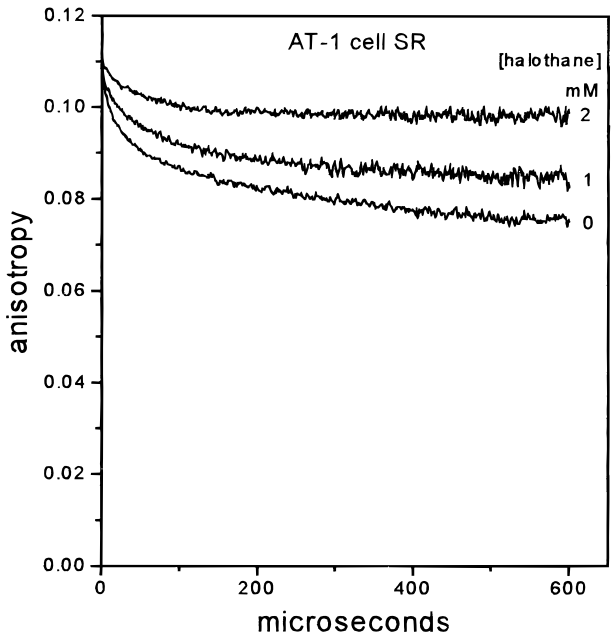

FIGURE 5: Influence of halothane on phosphorescence anisotropy decay of ERITC-labeled SR from AT-1 cardiomyocytes.

TPA response of cardiac Ca-ATPase to hexanol being different from the response of skeletal SR Ca-ATPase.

Effects of Halothane and Diethyl Ether on TPA of Cardiac SR and SR from AT-1 Atrial Myocytes. We wanted to know whether the differential response of cardiac vs skeletal SR Ca-ATPase to hexanol was peculiar to hexanol or was shared by other general anesthetics. Previous work in this laboratory showed that the TPA responses to halothane of ERITC-labeled cardiac SR (*7*) and skeletal SR (*4*) differ markedly in ways similar to the responses of cardiac and skeletal SR to hexanol. To determine whether the different response of cardiac SR Ca-ATPase to halothane might be due to the presence of phospholamban in cardiac SR, we investigated the influence of halothane on the TPA decay of ERITC-labeled AT-1 cell SR. Halothane at 1 and 2 mM markedly slows the TPA decay of ERITC-labeled AT-1 cell SR (Figure 5) and increases the value of r_∞. These responses to halothane are qualitatively and quantitatively similar to the effects of halothane on TPA of ERITC-labeled cardiac SR (*7*) but very different from the responses of ERITC-labeled skeletal SR to halothane (*4*), where no significant changes in r_∞ were observed in response to halothane at concentrations up to 7 mM.

Diethyl ether at concentrations from 0.3 to 0.6 M slows the rate of TPA decay and increases the value of r_∞ of ERITC-labeled cardiac SR (Figure 6A) and AT-1 cell SR (Figure 6B). These responses are quite different from the responses of ERITC-labeled skeletal SR to diethyl ether (*3*), where these levels of diethyl ether increase the rate of TPA decay but do not significantly change r_∞.

ERITC-labeled Ca-ATPase of cardiac SR and AT-1 cell SR responds to hexanol, halothane, and ether similarly: with slowed TPA decay and large increases in r_∞. These responses are quite different from the responses of ERITC-labeled Ca-ATPase of skeletal SR to these general anesthetics. These data support the conclusion that the differential response to these three general anesthetics is not due to the presence of phospholamban in cardiac SR.

Influence of Hexanol and Diethyl Ether on TPA of ERIA-Labeled Cardiac SR. It is possible that the changes in the TPA responses that we observe in response to general anesthetics are due to an artifact of labeling the Ca-ATPase with ERITC or to some peculiar property of ERITC-labeled cardiac SR Ca-ATPase relative to ERITC-labeled Ca-ATPase of skeletal SR. Moreover, despite the results of fitting the uniaxial rotation model to our data (Figure 3), the changes in r_∞ that we observe cannot be unequivocally attributed to an increase in the proportion of oligomers that are too large to rotate appreciably on the millisecond time scale. They might be due to changes in the probe angles, as described by eq 5. To investigate these possibilities, we determined the TPA responses of cardiac SR labeled with ERIA. In SERCA1 Ca-ATPase, ERIA probably labels a pair of cysteines (*34*) that are more than 150 residues away from the lysine where ERITC is believed to bind.

Cardiac SR labeled with ERIA shows slower TPA decays and increases in r_∞ in response to both hexanol (Figure 7A) and diethyl ether (Figure 7B). These responses are qualitatively similar to those we found with ERITC-labeled cardiac SR. If the cardiac Ca-ATPase undergoes a conformational change in response to general anesthetics, it seems unlikely that the changes in probe angles would be rather similar for two different phosphorescent chromophores located at some distance from one another on the protein.

The results with ERIA-labeled cardiac SR support the interpretations that (1) the different TPA response of cardiac SR to general anesthetics is not due to an artifact of ERITC labeling and (2) the formation of large, immobile oligomers, rather than probe angle changes, is probably responsible for the increases in r_∞ in cardiac SR in response to general anesthetics. A *caveat* for this interpretation is that ERIA significantly labels other proteins besides the Ca-ATPase in cardiac SR (Figure 1D).

Influence of Increased Ionic Strength on the TPA Responses of Cardiac SR to Hexanol. Electrostatic interactions have been implicated in the formation of large oligomers of

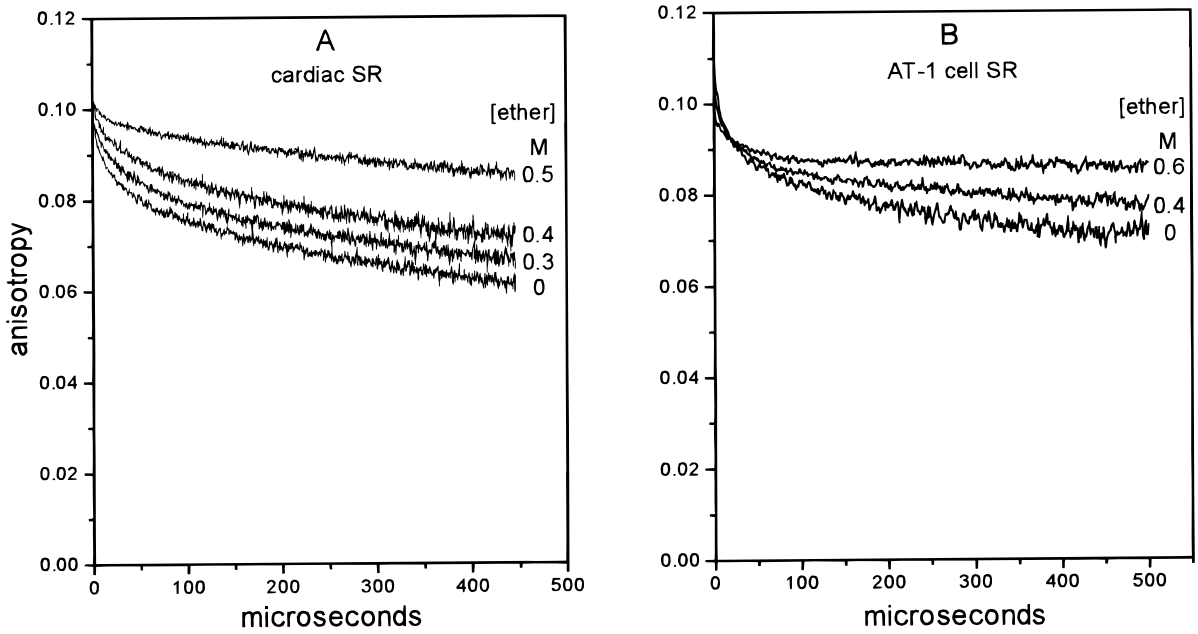

FIGURE 6: Influence of diethyl ether on phosphorescence anisotropy decay of ERITC-labeled cardiac SR (A) and of ERITC-labeled SR from AT-1 cardiomyocytes (B).

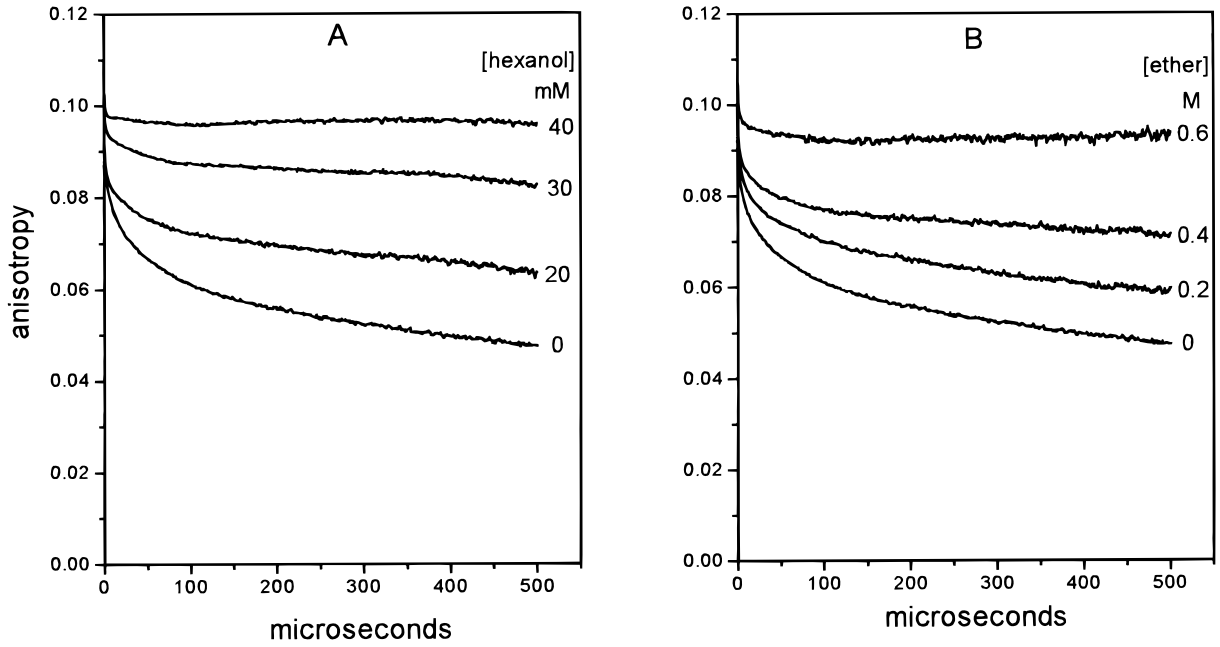

FIGURE 7: Influence of hexanol (A) and diethyl ether (B) on phosphorescence anisotropy decay of ERIA-labeled cardiac SR.

Ca-ATPase of skeletal and cardiac SR in response to melittin (*8*, *11*) and polycations (*11*, *35*). If electrostatic interactions contribute to the formation of large oligomers of SERCA2a Ca-ATPase in response to general anesthetics, then increasing the ionic strength of the medium would be expected to diminish the proportion of large oligomers formed.

We investigated the effects of increasing ionic strength with LiCl on the effect of hexanol on TPA of ERITC-labeled cardiac SR. In the absence of hexanol, 1 M LiCl increased the speed of TPA decay and decreased the value of r_∞ (Figure 8). The TPA response to 30 mM hexanol, slower TPA decay and increased r_∞, was markedly enhanced by 1 M LiCl (Figure 8). In a similar experiment with 0.5 M LiCl (data not shown), the effects of LiCl, in both the presence and the absence of hexanol, were qualitatively similar to, but smaller in magnitude than, those of 1 M LiCl. These results are consistent with the interpretation that electrostatic attraction contributes to the formation of large oligomers in the absence of hexanol but that electrostatic effects inhibit the formation of large oligomers in response to hexanol.

Influence of General Anesthetics on the Ca-ATPase Activity of Cardiac and Skeletal SR. Previous results from this laboratory have shown that the formation of large oligomers of Ca-ATPase is commonly associated with decreased Ca-ATPase activity, both in skeletal and in cardiac SR. These effects have been observed in response to local anesthetics (*6*, *7*), melittin (*8*, *9*, *11*), and polycations (*11*). We wanted to determine whether the formation of large oligomers of Ca-ATPase of cardiac SR in response to general anesthetics is also associated with diminished Ca-ATPase activity.

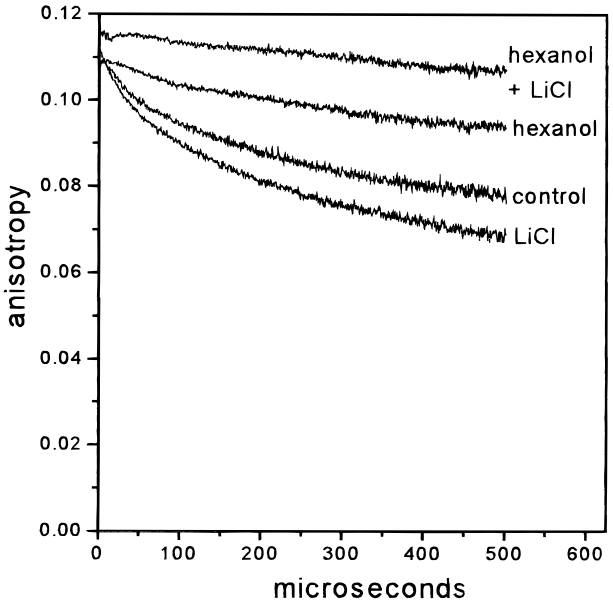

FIGURE 8: Effect of increasing ionic strength with 1 M LiCl on the phosphorescence anisotropy decay of ERITC-labeled cardiac SR in the presence and absence of 30 mM hexanol. The curve labeled control was obtained with neither hexanol nor LiCl.

Effect of Hexanol on Ca-ATPase Activity. The effect of preincubation with hexanol on the Ca-ATPase activity of cardiac and skeletal SR was determined for several different levels of free Ca^{2+} (Figure 9). While there are minor differences in the responses of cardiac and skeletal SR to hexanol, the effects of hexanol on Ca-ATPase activity over a wide range of pCa are remarkably similar in cardiac and skeletal SR. The results for skeletal SR are consistent with our previous results (*6*) and with results of others (*36*−*38*). The similarity of the responses of skeletal and cardiac Ca-ATPase activity to hexanol stands in contrast to the striking differences we observed in the effects of hexanol on the phosphorescence anisotropy decays of ERITC-labeled cardiac and skeletal SR. Concentrations of hexanol (20 and 30 mM) that cause significant increases in r_∞ in cardiac SR labeled with ERITC or with ERIA markedly stimulate Ca-ATPase activity. This was an unexpected result since other perturbations we had previously studied that led to the formation of large oligomers of Ca-ATPase were associated with decreased enzymatic activity of the protein.

Effect of Halothane on Ca-ATPase Activity. We compared the influences of halothane on the Ca-ATPase activities of skeletal and cardiac SR (Figure 10A,B) at pCa 5.5 under almost identical conditions. The effects of halothane on the Ca-ATPase activity of skeletal SR are rather similar to their effects on cardiac SR. Lower concentrations stimulate the Ca-ATPase activities of both SR preparations, and higher concentrations tend to inhibit enzyme activity. One difference is that the stimulation of the Ca-ATPase of cardiac SR by 3.5 mM halothane is much less than the stimulation of Ca-ATPase activity of skeletal SR by this concentration of halothane (*15*). The biphasic effects of halothane, stimulation of Ca-ATPase activity at low levels of halothane and inhibition of Ca-ATPase at higher levels, were previously demonstrated in skeletal SR (*4*, *39*−*41*). The effects of halothane on cardiac SR have been reported to depend on $[Ca^{2+}]$ and on pH and will be discussed further below.

Influence of Diethyl Ether on Ca-ATPase Activity. The response of Ca-ATPase activities of skeletal and cardiac SR (Figure 10C,D) were similar. Diethyl ether, at 0.2−0.4 M, significantly stimulated Ca-ATPase activity. At concentrations above 0.4 M ether, Ca-ATPase activity declined. Stimulation of Ca-ATPase in skeletal SR by diethyl ether had been previously reported (*42*−*45*). Low levels of diethyl ether (6−24 mM) were reported to have no significant effect on the Ca-ATPase activity of cardiac SR (*46*).

In cardiac SR, Ca-ATPase activities are enhanced by levels of hexanol, halothane, and diethyl ether that promote the formation of large, immobile oligomers of the Ca-ATPase. This suggests that large oligomers of cardiac Ca-ATPase that form in response to general anesthetics are different from the large oligomers that form in response to local anesthetics, melittin, and polycations, since in response to these compounds, Ca-ATPase activity is dramatically inhibited.

DISCUSSION

Overview. This study began with the observation that the TPA response of ERITC-labeled cardiac SR to hexanol, slower TPA decay and increased r_∞, was qualitatively different from that of ERITC-labeled skeletal SR. The major purpose of this study is to investigate the basis for the different TPA behavior of cardiac SR. As described above, our data support the following interpretations: (1) the difference in TPA response is not peculiar to hexanol but is shared by halothane and diethyl ether; (2) the presence of phospholamban in cardiac SR is not responsible for the different TPA response of cardiac SR to these three general anesthetics; (3) the different TPA response of cardiac SR compared to skeletal SR is not an artifact produced by labeling with ERITC; (4) the increases in r_∞ in cardiac SR in response to general anesthetics are due to increases in the proportion of very large oligomers, rather than to changes in probe angles; (5) electrostatic forces do not promote the formation of large oligomers of cardiac SR in response to hexanol; and (6) the formation of large oligomers in cardiac SR in response to the three general anesthetics may be associated with increased activity of cardiac Ca-ATPase; thus the large oligomers that form in cardiac SR in response to general anesthetics are different from those that form in response to local anesthetics, melittin, and polycations, which are enzymatically inactive.

Effects of Halothane on the Ca-ATPase of Cardiac SR. The effects of halothane on the Ca-ATPase of cardiac SR are complex and deserve further discussion. Halothane has been reported to stimulate and to inhibit Ca-ATPase and Ca^{2+} uptake of cardiac SR (*7*, *15*, *46*−*48*) depending on experimental conditions. The effects of halothane on Ca-ATPase of cardiac SR appear to be profoundly pH-dependent: halothane was reported to stimulate Ca^{2+} uptake at pH above 7.0 but to inhibit uptake at pH below 7.0 (*49*). The effects of halothane on Ca-ATPase of cardiac SR also depend on the free Ca^{2+} concentration. The inhibitory effect of halothane on cardiac SR Ca-ATPase appears to be competitive with respect to Ca^{2+} (*15*, *50*). At high Ca^{2+} levels (20−100 μM), clinical levels of halothane have little effect on Ca-ATPase activity. By contrast, at low Ca^{2+} levels (0.15 μM), cardiac Ca-ATPase activity is markedly inhibited by clinical levels of halothane (*7*, *15*, *50*). At low Ca^{2+}, we

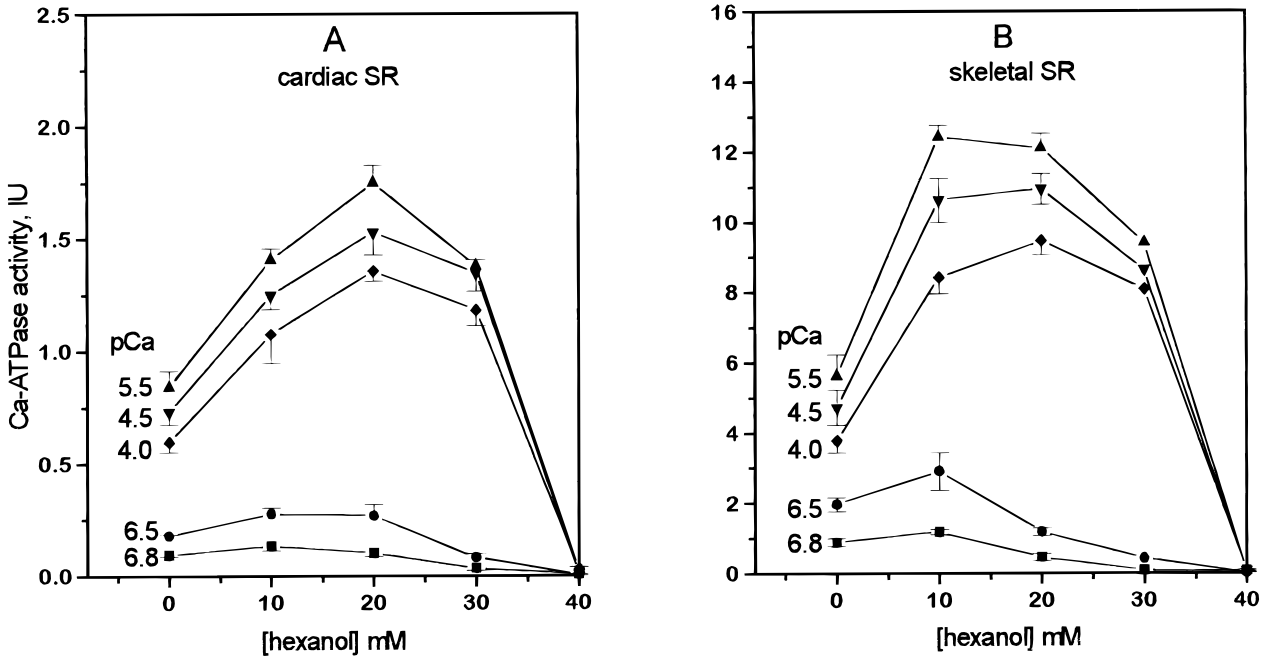

FIGURE 9: Effect of hexanol on Ca-ATPase activity of cardiac SR (A) and skeletal SR (B) over a range of free Ca^{2+} concentrations, indicated by the pCa values shown to the left of the curves.

have found that cardiac and skeletal SR Ca-ATPase activities are oppositely affected by halothane: skeletal Ca-ATPase activity is stimulated, but cardiac SR is inhibited by 2 mM halothane (*15*). This differential response to halothane at low levels of Ca^{2+} was also observed in SERCA1 (fast skeletal) and SERCA2a (cardiac) isoforms of Ca-ATPase expressed in Sf21 cells, showing that phospholamban is not responsible for the difference. We concluded that the SERCA2a Ca-ATPase isoform responds to halothane differently from the SERCA1 isoform (*15*).

Possible Explanations for the Differential TPA Response of the Ca-ATPases of Cardiac and Skeletal SR to General Anesthetics. Among the differences between cardiac and skeletal SR that might account for their differing responses to general anesthetics are (a) differences in membrane lipids, (b) differences in membrane proteins (other than phospholamban), or (c) differences between the SERCA2a (cardiac) and SERCA1 (fast skeletal) isoforms of Ca-ATPase.

Differences in Membrane Lipids. The membrane lipids of SR from rabbit fast skeletal muscle are similar to the lipids of SR from dog heart in phospholipid-to-protein ratio, in the fraction of saturated, unsaturated, and branched fatty acyl chains, and in lipid order parameters estimated from spin-labeled stearic acid derivatives (*51*). There is a significantly higher level of cholesterol in rabbit skeletal SR than in canine cardiac SR. The apparent compositional and physical similarity of membrane lipids in cardiac and skeletal SR (*51*) argues against differences in membrane lipids as the source of the differing responses of cardiac and skeletal SR, but this explanation cannot be ruled out entirely.

Differences in Membrane Proteins. There is more Ca-ATPase in SR from rabbit fast skeletal SR (about 75% of membrane protein) than in SR from canine ventricular myocardium (about 25% of membrane protein). Despite the lower concentration of Ca-ATPase in the cardiac SR membrane, the apparent fraction of very large oligomers of Ca-ATPase that are too large to rotate on the millisecond time scale) is much higher in cardiac SR (*13*, *14*, *51*). The presence of phospholamban is apparently not responsible for the high proportion of very large oligomers in cardiac SR (our data; ref *14*). This is consistent with the view that the Ca-ATPase in cardiac SR has a greater propensity to form large oligomers than Ca-ATPase in skeletal SR. Our data argue strongly against the presence of phospholamban in cardiac SR as the source of the different TPA responses to general anesthetics. We cannot rule out the possibility that some other protein that is present in cardiac SR, but not in skeletal, or vice versa, is responsible for the different TPA responses of cardiac vs skeletal SR to general anesthetics.

Differences between SERCA1 and SERCA2a. Our recent research (*15*) shows that the differential response of SERCA1 and SERCA2a to halothane at low (0.15 μM) free Ca^{2+} is due to a functional difference between the two isoforms. This suggests that the increase in large oligomers of Ca-ATPase in response to general anesthetics that occurs in cardiac SR but not in skeletal SR may also be due to a difference between the SERCA2a and the SERCA1 isoforms. To test this possibility we should express the SERCA1 and SERCA2a isoforms in the same cell line at high enough levels to allow TPA measurements. We do not currently have this capability, but it is a goal of our research.

Stimulation of Ca-ATPase Activity by Lower Levels of General Anesthetics. General anesthetics have been shown to increase the fluidity of the acyl chain regions of a host of biological membranes (*52*, *53*). We have previously observed correlations between the effects of general anesthetics on the fluidity of the membrane of skeletal SR and the effects on Ca-ATPase activity in response to diethyl ether (*3*, *45*) hexanol (*6*), and halothane (*4*). The correlations between membrane fluidity and Ca-ATPase activity and between membrane fluidity and the rotational mobility of the Ca-ATPase suggest that high enzymatic activity requires that the environment of the Ca-ATPase must be sufficiently fluid to permit specific protein motions that are involved in

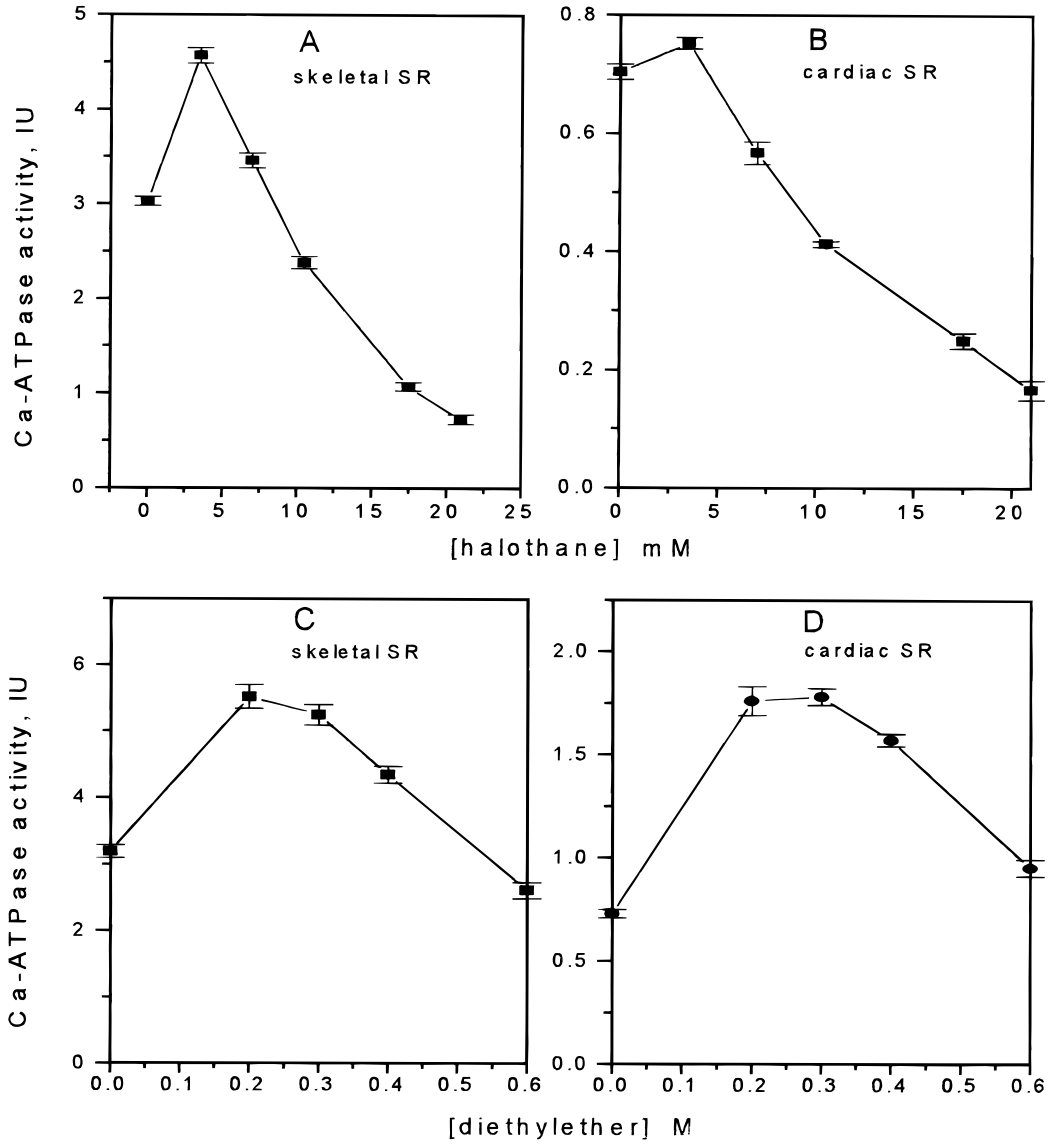

FIGURE 10: Influence of halothane (A,B) and diethyl ether (C,D) on Ca-ATPase activity of skeletal and cardiac SR.

catalysis (*54*). We believe that the stimulation of Ca-ATPase activity in both skeletal and cardiac SR at lower concentrations of hexanol, halothane, and diethyl ether is due to the increase in membrane fluidity caused by the general anesthetics. At lower concentrations of the general anesthetics, under the conditions of our experiments, it appears that the stimulation of Ca-ATPase activity due to increased membrane fluidity outweighs inhibitory effects of the anesthetics acting directly on the Ca-ATPase or via other mechanisms.

Molecular Mechanisms for the Differential TPA Response of Cardiac and Skeletal SR Ca-ATPases to General Anesthetics. Our previous results have been consistent with the view that conditions that promote the formation of very large (immobile) oligomers of Ca-ATPase, both in skeletal and in cardiac SR, are associated with inhibition of Ca-stimulated ATPase activity. Among the perturbations that cause the formation of large oligomers and inhibit Ca-ATPase activity are local anesthetics (lidocaine) in skeletal (*6*) and cardiac (*7*) SR, the inhibitors thapsigargin (*12*) and cyclopiazonic acid (*5*) in skeletal SR, and melittin and polycations in skeletal SR (*10*, *11*).

Many of the data in the present paper are *not* consistent with a correlation between inhibition of Ca-ATPase activity and the formation of very large oligomers of Ca-ATPase. In cardiac SR, the general anesthetics hexanol, halothane, and diethyl ether, at lower concentrations, all stimulate Ca-ATPase activity while promoting formation of very large oligomers. (At higher concentrations, the general anesthetics inhibit Ca-ATPase activity while promoting the formation of still higher proportions of very large Ca-ATPase oligomers.) How can these discrepancies between the present results and our previous observations be explained? What accounts for the differential responses of the oligomeric states of skeletal and cardiac Ca-ATPases to general anesthetics?

Formation of Large Oligomers of Ca-ATPase in Response to Agents That Stabilize E2 Conformers of Ca-ATPase. Thapsigargin and cyclopiazonic acid are specific inhibitors of SERCA-type Ca-ATPases. Thapsigargin enhances the proportion of E2 conformers in skeletal SR (*55*−*58*) and promotes formation of very large oligomers of Ca-ATPase (*12*). Cyclopiazonic acid also favors E2 conformations and very large Ca-ATPase oligomers in skeletal SR (*5*). Melittin inhibits Ca-ATPase in skeletal SR and promotes formation of very large oligomers of Ca-ATPase (*11*). Melittin preferentially interacts with the E2 form of the Ca-ATPase to stabilize E2 and to prevent the E2 to E1 transition (*11*).

There is evidence that E2 conformations of Ca-ATPase have a greater tendency to form large oligomers than do E1 conformations. Vanadate, which stabilizes an E2-P-like conformation of Ca-ATPase, has been shown to promote the formation of two-dimensional crystals of Ca-ATPase (*59*). Thapsigargin also causes formation of two-dimensional crystals of Ca-ATPase (*60*).

We believe that both the formation of large oligomers of Ca-ATPase in response to thapsigargin and cyclopiazonic acid and the inhibition of Ca-ATPase activity by these agents are consequences of stabilization of E2 conformers of the enzyme. Thus inhibition of enzymatic activity does not appear to be caused by the formation of large oligomers.

Formation of Large Oligomers of Ca-ATPase and Inhibition of Ca-ATPase Activity in Response to Polycations and Local Anesthetics. Both the formation of large oligomers and inhibition of Ca-ATPase activity by polycations can be reversed by increased ionic strength (*11*, *35*). It thus appears that an electrostatic mechanism is primarily responsible for the formation of large oligomers. The formation of large oligomers and the inhibition of Ca-ATPase activity caused by lidocaine cannot be reversed by increased ionic strength (Kutchai, unpublished results). The mechanism whereby lidocaine causes large oligomers to form in both skeletal (*6*) and cardiac SR (*7*) remains to be elucidated. Further research will be required to determine whether the formation of large oligomers of Ca-ATPase in response to polycations and local anesthetics is causally related to inhibition of Ca-ATPase activity by these compounds.

Formation of Large Oligomers in Cardiac SR, but Not in Skeletal SR, in Response to General Anesthetics. What is responsible for the formation of large oligomers of Ca-ATPase in cardiac SR in response to general anesthetics? Why does this not occur in skeletal SR?

We believe that the differential responses of cardiac and skeletal SR in our time-resolved phosphorescence experiments may be due to the promotion of E2 conformations by general anesthetics in cardiac SR, but not in skeletal SR. Studies of the fluorescence of FITC-labeled cardiac SR in response to halothane (*7*) support the interpretation that halothane stabilizes E2 conformations of the cardiac Ca-ATPase. Recently, we compared the responses of FITC-labeled skeletal and cardiac SR to halothane and determined the effects of halothane on formation of E2-P from inorganic phosphate in skeletal and cardiac SR (*15*). The results suggest that the stabilization of E2 conformers, especially of the E2-P conformation, by halothane is much more pronounced in cardiac SR than in skeletal SR. It is our working hypothesis that the differential formation of large oligomers in cardiac SR in response to general anesthetics is due to a greater stabilization of E2 conformers in cardiac SR than in skeletal SR. Further research is required to test this hypothesis.

Conclusions. The research presented here shows that the relationships between the oligomeric state of SR Ca-ATPases and their ATPase activities are more complex than have been previously appreciated. There may be multiple mechanisms that lead to formation of large oligomers and inhibition of Ca-ATPase activity. Further research will be necessary to determine whether, in response to a particular treatment, there is a causal relationship between the formation of large oligomers and inhibition of Ca-ATPase activity. Moreover, our results suggest that there are significant differences between the Ca-ATPases of skeletal and cardiac SR in their responses to general anesthetics. The data are consistent with the interpretation that these represent differences between the SERCA1 and SERCA2a isoforms, but testing this hypothesis will require additional research.

ACKNOWLEDGMENT

We are pleased to acknowledge the assistance of Yongli Shi in performing some of the experiments, and we wish to thank Drs. Razvan Cornea, Greg Hunter, Brad Karon, James Mahaney, and Laxma Reddy for commenting on the manuscript. Dr. Min Zhao provided advice about labeling Ca-ATPase with ERIA. Dr. Bruce Gaylinn and Ron Pace provided advice and assistance in use of the Fluorimager and Image-Quant software.

REFERENCES

1. Thomas, D. D., and Karon, B. S. (1994) in *The Temperature Adaptation of Biological Membranes* (Cossins, A. R., Ed.) pp 1−12, Portland Press, London.
2. Cornea, R., and Thomas, D. D. (1994) *Biochemistry 33*, 2912−2920.
3. Birmachu, W., and Thomas, D. D. (1990) *Biochemistry 29*, 3904−3914.
4. Karon, B. S., and Thomas, D. D. (1993) *Biochemistry 32*, 7503−7511.
5. Karon, B. S., Mahaney, J. E., and Thomas, D. D. (1994) *Biochemistry 33*, 13928−13937.
6. Kutchai, H., Mahaney, J. E., Geddis, L. M., and Thomas, D. D. (1994) *Biochemistry 33*, 13208−13222.
7. Karon, B., Geddis, L. M., Kutchai, H., and Thomas, D. D. (1995) *Biophys. J. 68*, 936−945.
8. Mahaney, J. E., and Thomas, D. D. (1991) *Biochemistry 30*, 7498−7506.
9. Mahaney, J. E., Kleinschmidt, J., Marsh, D., and Thomas, D. D. (1992) *Biophys. J. 63*, 1513−1522.
10. Voss, J., Hussey, D., Birmachu, W., and Thomas, D, D. (1991) *Biochemistry 30*, 7498−7506.
11. Voss, J. C., Mahaney, J. E., and Thomas, D. D. (1995) *Biochemistry 34*, 930−939.
12. Mersol, J. V., Kutchai, H., Mahaney, J. E., and Thomas, D. D. (1995) *Biophys. J. 68*, 208−215.
13. Voss, J., Jones, L. R., and Thomas, D. D. (1994) *Biophys. J. 67*, 190−196.
14. Voss, J. C., Mahaney, J. E., Jones, L. R. and Thomas, D. D. (1995) *Biophys. J. 68*, 1787−1795.
15. Karon, B. S., Autry, J. M., Shi, Y., Garnett, C. E., Inesi, G., Jones, L. R., Kutchai, H., and Thomas, D. D. (1997) *J. Biol. Chem.*, submitted for publication.
16. Fabiato, A. (1988) *Methods Enzymol. 157*, 378−417.
17. Fernandez, J. L., Rosembatt, M., and Hidalgo, C. (1980) *Biochim. Biophys. Acta 599*, 552−568.
18. Feher, J. J., and Briggs F. N. (1983) *Biochim. Biophys. Acta 727*, 389−402.
19. Jones, L. R., and. Cala, S. E. (1981) *J. Biol. Chem. 256*, 11809−11818.
20. Field, L. J. (1988) *Science 239*, 1029−1033.
21. Jones, L. R., and Field. L. J. (1993) *J. Biol. Chem. 268*, 11486-11488.
22. Gornall, A. G., Bardawill, C. J., and David, M. M. (1949) *J. Biol. Chem. 177*, 751−766.
23. Lowry, O. H., and Passonneau, J. V. (1972) *A flexible system of enzymatic analysis*, pp 146−148, Academic Press, New York.
24. Zhao, M. (1997) Molecular dynamics of calcium pumping and regulation in skeletal and skeletal and cardiac sarcoplasmic reticulum, Doctoral Dissertation, p 30, University of Minnesota, Minneapolis, MN.

25. Eads, T. M., Thomas, D. D., and Austin, R. H. (1984) *J. Mol. Biol. 179*, 55−81.
26. Ludescher, R. D., and Thomas, D. D. (1988) *Biochemistry 27*, 3343−3351.
27. Bevington, P. R. (1969) *Data Reduction and Error Analysis for the Physical Sciences*, McGraw-Hill, New York.
28. Belford, G. G., Belford, R. L., and Weber, G. (1972) *Proc. Natl. Acad. Sci. U.S.A. 69*, 1392−1393.
29. Szabo, A. (1984) *J. Chem. Phys. 81*, 150−166.
30. Tada, M., and Katz. A. M. (1982) *Annu. Rev. Physiol. 44*, 401−423.
31. Tada, M., Yamada, M., Kadoma, M., Inui, M., and Ohmori, F. (1982) *Mol. Cell. Biochem. 46*, 73−95.
32. Inui, M., Chamberlain, B. K., Saito, A., and Fleischer, S. (1986) *J. Biol. Chem. 261*, 1794−1800.
33. James, P. M., Inui, M., Tada, M., Chiesi, M., and Carafoli, E. (1989) *Nature 342*, 90−92.
34. Bishop, J. E., Squier, T. C., Bigelow, D. J., and Inesi, G. (1988) *Biochemistry 27*, 5233−5240.
35. Xu, Z., and Kirchberger, M. A., (1989) *J. Biol. Chem. 264*, 16644−16651.
36. Kondo, M., and Kasai, M. (1973) *Biochim. Biophys. Acta 311*, 391−399.
37. Hara, K., and Kasai, M. (1977) *J. Biochem. 82*, 1005−1017.
38. Melgunov, V. I., Jindals, S., and Belikova, M. P. (1987) *Biokhimiya 52*, 1688−1695.
39. Nelson, T. E., and Sweo, T. (1988) *Anesthesiology 69*, 571−577.
40. Blanck, T. J. J., Peterson, C. V., Boroody, B., Tegazzin, V., and Lou, J. (1992) *Anesthesiology 76*, 813−821.
41. Louis, C. F., Zaulkernan, K., Roghair, T., and Mickelson, J. R. (1992) *Anesthesiology 77*, 114−125.
42. Inesi, G., Goodman, J. J., and Watanabe, S. (1967) *J. Biol. Chem. 242*, 4637−4643.
43. Salama, G., and Scarpa, A. (1980) *J. Biol. Chem. 255*, 6525−6528.
44. Kidd, P., Scales, D., and Inesi, G. (1981) *Biochim. Biophys Acta 645*, 124−131.
45. Bigelow, D. J., and Thomas, D. D. (1987) *J. Biol. Chem. 262*, 13449−13456.
46. Lain, R. F., Hess, M. L., Gertz, E. W., and Briggs, F. N. (1968) *Circ. Res. 23*, 597−604.
47. Blanck, T. J. J., Gruener, R., Suffecool, S. L., and Thompson, M. (1981) *Anesth. Analg. (N.Y.) 60*, 492−498.
48. Frazer, M. J., and Lynch, C., III (1992) *Anesthesiology 77*, 316−323.
49. Casella, E. S., Suite, N. D. A., Fisher, Y. I., and T. J. J. Blanck (1987) *Anesthesiology 67*, 386−390.
50. Malconico, S. M., and McCarl, R. L. (1982) *Mol. Pharm. 22*, 8−10.
51. Birmachu, W., Voss, J. C., Louis, C. F., and Thomas, D. D. (1993) *Biochemistry 32*, 9445−9453.
52. Trudell, J. R. (1991) in *Drug and Anesthetic Effects on Membrane Structure and Function* (Aloia, R. C., Curtain, C. C., and Gordon, L., Eds.) pp 1−14, Wiley-Liss, New York.
53. Firestone, L. L., and Kitz, R. J. (1986) *Semin. Anesth. 5*, 286−300.
54. Squier, T. C., Bigelow, D. J., and Thomas, D. D. (1988) *J. Biol. Chem. 263*, 9178−9186.
55. Saraga, Y., Wade, J. B., and Inesi, G. (1992) *J. Biol. Chem. 267*, 1286−1292.
56. Sagara, Y., Fernandez-Belda, F., de Meis, L., and Inesi, G. (1992) *J. Biol. Chem. 267*, 12606−12613.
57. Wictome, M., Michelangeli, F., Lee, A. G., and East, J. M. (1992) *FEBS Lett. 304*, 109−113.
58. Wictome, M., Henderson, I., Lee, A. G., and East, J. M. (1992) *Biochem. J. 283*, 525−529.
59. Dux, L., and Martonosi, A. N. (1983) *J. Biol. Chem. 258*, 10111−10115.
60. Stokes, D. L., and Lacapere, J. J. (1994) *J. Biol. Chem. 269*, 11606−11613.
61. Laemmli, U. K. (1970) *Nature (London) 227*, 680−685.

BI9722002